Evidence for serpentinization of the forearc mantle wedge along the Nicoya Peninsula, Costa Rica

Heather R. DeShon[1,2] and Susan Y. Schwartz[1]

[1]   Characterizing the hydration state of the forearc mantle wedge yields valuable information on frictional stability at the downdip edge of subduction megathrusts. Simultaneous inversion of P- and S-wave arrival times collected as part of the Costa Rica Seismogenic Zone Experiment yields 1D and 3D P- and S-wave velocity models (V_P and V_S) for the Nicoya Peninsula segment of the Middle America Trench. Nicoya Peninsula 1D velocity models show similar velocity gradients to country-wide 1D velocity models from $5-30$ km depth but diverge at expected Moho depths due to proximity to the subducting Cocos plate. 3D V_P values range from $7.2-7.6$ km/sec in the forearc mantle wedge. Receiver functions computed at Global Seismic Network station JTS in northwestern Costa Rica confirm these V_P values, yield V_P/V_S of ~1.85, and place the continental Moho at 36 ± 4 km depth. V_P and V_P/V_S are consistent with $15-25\%$ serpentinization of the forearc mantle wedge.   INDEX TERMS: 7230 Seismology: Seismicity and seismotectonics; 7223 Seismology: Seismic hazard assessment and prediction; 8015 Structural Geology: Local crustal structure; 8105 Tectonophysics: Continental margins and sedimentary basins (1212); 8180 Tectonophysics: Tomography. **Citation:** DeShon, H. R., and S. Y. Schwartz (2004), Evidence for serpentinization of the forearc mantle wedge along the Nicoya Peninsula, Costa Rica, *Geophys. Res. Lett.*, *31*, L21611, doi:10.1029/2004GL021179.

1.   Introduction

[2]   Most large and great ($M_w > 7$) underthrusting earthquakes nucleate within the shallow, frictionally unstable portion of the subduction megathrust termed the seismogenic zone. Determining the downdip, and commonly landward, extent of potential rupture during such events is necessary for accurate seismic hazard assessment. Conditional stability regimes may exist along the updip and downdip limits of the transition from pure stick-slip to aseismic behavior [*Scholz*, 1998]. For low temperature and subduction zones with thin crust in the overlying plate, *Hyndman et al.* [1997] suggested that the downdip rupture extent depends on the hydration state of the forearc mantle wedge rather than on the temperature- and pressure-dependent onset of ductile behavior. Dehydration of oceanic slab components may hydrate continental mantle olivine and lead to the formation of serpentine minerals that exhibit both stable sliding and strain rate dependent conditional stability under laboratory conditions [e.g., *Hyndman and Peacock*, 2003]. Serpentinized mantle wedges have been identified in Chile, Alaska, Cascadia, and Japan [*Graeber and Asch*, 1999; *Kamiya and Kobayashi*, 2000; *Zhao et al.*, 1992; *Rondenay et al.*, 2001; *Seno et al.*, 2001] through recognition of decreased P- and S-wave seismic velocities, increased V_P/V_S, and reduced density [i.e., *Hyndman and Peacock*, 2003].

[3]   One goal of the Nicoya Peninsula Costa Rica Seismogenic Zone experiment (CRSEIZE) was to define the updip, downdip, and along-strike variability of microseismicity within a segment of the Middle America Trench (MAT) capable of generating $M_w \sim 7.7$ earthquakes (Figure 1). Initial studies of seismic velocity throughout Costa Rica indicated a large Moho velocity contrast at $35-45$ km depth with continental mantle $V_P \geq 7.8$ km/sec [*Matumoto et al.*, 1977; *Quintero and Kulhanek*, 1998; *Protti et al.*, 1996; *Sallarès et al.*, 2000]. Recent models using inversion techniques do not indicate a large Moho velocity contrast at these depths (Figure 2a) [*Quintero and Güendel*, 2000; *Quintero and Kissling*, 2001; *Husen et al.*, 2003]. Using wide-angle P-wave refraction data in the Nicoya Peninsula region, *Sallarès et al.* [2001] suggested the continental Moho dipped from 30 km depth at the subducting slab to 40 km depth inland and that decreased V_P (~7.4 km/sec) in the forearc mantle wedge was evidence of serpentinization. Constraining the depth to the continental Moho and the V_P and V_S structure of the forearc mantle wedge will improve seismic hazard assessment of the downdip rupture limit of large magnitude earthquakes in this region.

[4]   This study provides V_P and V_P/V_S models and continental Moho depth estimates for the Nicoya Peninsula using arrival time data recorded by a local on/offshore seismic array. We simultaneously invert P- and S-wave arrival times using the inversion program VELEST (version 3.1) [*Kissling et al.*, 1995] to compute 1D velocity models for the Nicoya Peninsula. We compare results to the local earthquake tomography-derived 3D V_P model using the Nicoya experiment dataset [*DeShon*, 2004]. In order to further constrain the location of and velocity contrast across the continental Moho near the Nicoya seismic array, we compute receiver functions of P-to-S conversions from teleseisms recorded at Global Seismic Network (GSN) station JTS (Figure 1).

2.   Nicoya Peninsula Minimum 1D Velocity Models

[5]   Minimum 1D velocity models with coupled station corrections [*Kissling*, 1988; *Kissling et al.*, 1995] have been successfully applied to heterogeneous regions such as subduction zones to interpret depth-variable velocity [e.g.,

[1]Earth Science Department and Institute of Geophysics and Planetary Physics, University of California, Santa Cruz, Santa Cruz, California, USA.

[2]Department of Geology and Geophysics, University of Wisconsin, Madison, Madison, Wisconsin, USA.
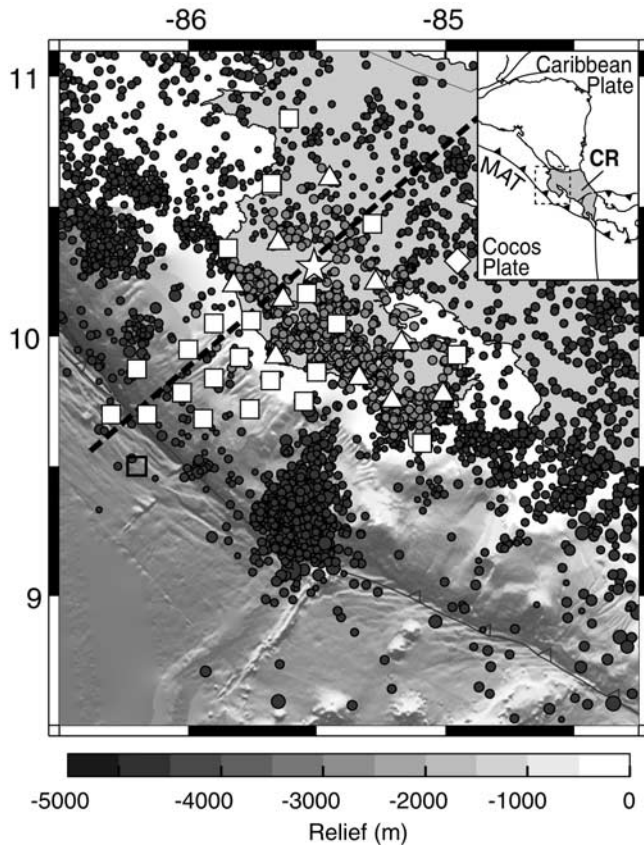
Figure 1. Nicoya Peninsula CRSEIZE location map. CR: Costa Rica; MAT: Middle America Trench; Black circles: initial earthquake locations through the global IASP91 model. Gray circles: earthquakes selected to invert for 1D *P*-wave structure. Triangles: short-period seismometers. Boxes: broad-band seismometers. Star: reference station GUAI. Diamond: GSN station JTS. White indicates stations used for 1D inversion. Dotted line: *P*-wave refraction data from *Sallarès et al.* [2001] and cross-section shown in Figure 3. Bathymetry from *von Huene et al.* [2000].

Kissling and Lahr, 1991; *Husen et al.*, 1999]. We follow the inversion calculation scheme of *Kissling et al.* [1995] to calculate minimum 1D velocity models. We choose 475 events with ≥ 8 *P*-wave arrivals, ≥ 6 *S*-wave arrivals, and a GAP (greatest azimuthal difference) $\leq 180°$, and we choose the centrally located broadband station, GUAI, as the 1D reference station (Figure 1). Inversions begin from a range of initial V_P models that include velocities consistent and inconsistent with the regional geology and that test a number of Moho depths; initial V_S models are calculated using constant V_P/V_S ratios of $1.60-1.90$ (Figure 2b). Layers with few earthquakes (<6 km and >40 km depth) are damped to maintain reasonable velocities in lower resolution regions. Further inversion details are described by *DeShon* [2004].

[6] Across the highest resolution depths (6–20 km), the Nicoya 1D V_P model agrees with the Costa Rica minimum 1D V_P model calculated using regional data [*Quintero and Kissling*, 2001]. Below ~30 km depth our model diverges from previous studies [i.e., *Protti et al.*, 1996; *Quintero and Kissling*, 2001], which reflects the influence of the

subducting slab and differences in earthquake datasets. Reference station GUAI lies directly above the subducting Cocos Plate, and the Nicoya 1D velocity model samples oceanic slab, oceanic mantle, and continental mantle between 30–40 km depth, near the expected intersection of the continental Moho and oceanic slab (Figure 3). V_P in the Nicoya 1D model at these depths ranges from 7.4–7.6 km/sec (Figure 2) and is consistent with expected subducting oceanic crust velocities or anomalously low continental mantle *P*-wave velocities. Due to the station geometry and data coverage of the Nicoya Peninsula CRSEIZE experiment resolution decreases significantly below 40 km depth, and normal mantle velocities ($V_P \sim 8.15$) in the local 1D model likely reflect oceanic mantle rather than continental mantle velocities.

[7] The range of the Nicoya minimum 1D V_S model and the average constant V_P/V_S value 1.78 is consistent with previous V_P/V_S values used to calculate V_S models for Costa Rica (Figure 2) [*Protti et al.*, 1996; *Yao et al.*, 1998; *Quintero and Güendel*, 2000].

3. Nicoya 3D Tomography Models

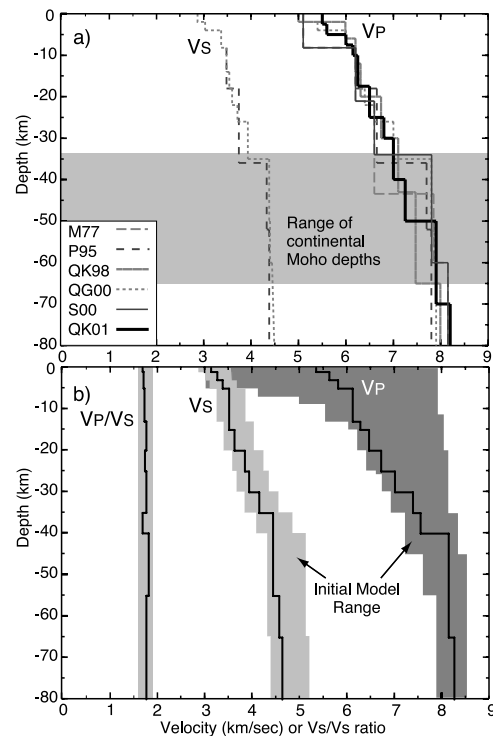[8] *DeShon* [2004] simultaneously inverted *P*-wave arrivals from 618 well-constrained earthquakes recorded

Figure 2. 1D V_P, V_S, and V_P/V_S models for Costa Rica. a) 1D velocity models from other studies. M77: *Matumoto et al.* [1977]; P95: *Protti et al.* [1995] for the Nicoya Gulf region; QK98: *Quintero and Kulhanek* [1998] based on Pn arrivals; QG00: *Quintero and Güendel* [2000]; S00: *Sallarès et al.* [2000]; QK01: *Quintero and Kissling* [2001] minimum 1D V_P model. When estimated, the studies use constant V_P/V_S of 1.78. b) Nicoya Peninsula minimum 1D velocity models (black lines) and initial model range used for inversion (shaded). Variable V_P/V_S averages 1.78.
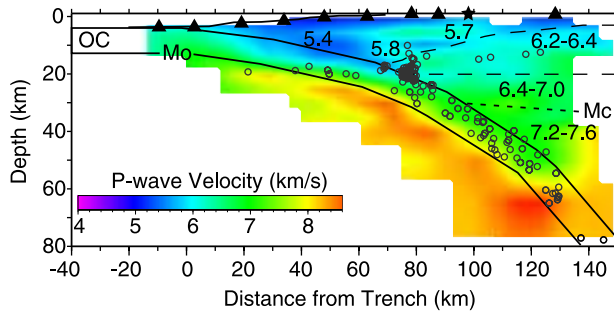
Figure 3. Cross-section through 3D V_P model shown with P-wave velocities and interpreted crustal structure [modified from *DeShon*, 2004]. Mc and Mo represent the continental and oceanic Moho respectively. OC: Cocos plate oceanic crust. Star: reference station GUAI. Open circles: seismicity within 8 km of cross-section. Cross-section location shown in Figure 1.

by Nicoya Peninsula CRSEIZE stations and JTS and derived a 3D V_P model for the Nicoya Peninsula region using the local earthquake tomography algorithm SIMULPS [i.e., *Evans et al.*, 1994]. The minimum 1D velocity model served as initial starting model, and inversion followed a coarse-to-fine progressive inversion scheme [e.g., *Husen et al.*, 2003]. The final model uses 10×10 km^2 mapview grid spacing and variable depth grid spacing following the 1D velocity model. Broad-scale crustal structure agrees with P-wave refraction data for the region [*Sallarès et al.*, 2001], and results for the forearc mantle region are summarized here.

[9] In northern Costa Rica, the continental Moho intersects the slab between $30-34$ km depth, and mantle wedge V_P ranges between $7.2-7.6$ km/sec (Figure 3). Continental Moho estimates consider velocity and earthquake location, but Moho location error is poorly constrained due to the low velocity contrast across the boundary. *Sallarès et al.* [2001] reported forearc mantle $V_P \sim 7.4-7.5$ km/sec in this region, and 3D V_P agrees with their 2D crustal structure and forearc mantle velocity estimate.

4. Receiver Functions

[10] To further constrain the location and velocity contrast across the continental Moho, we compute receiver functions of P-to-S conversions from teleseisms recorded at GSN station JTS (Figure 1). As part of a larger study of receiver functions for the Nicoya CRSEIZE array, we focus on the time period $1998-2002$ spanning the CRSEIZE experiment, and data selection is limited to $M_w \geq 5.8$ earthquakes that exhibit clean P-wave arrivals, low energy transverse components, and high signal-to-noise ratio (Figure 4). Data processing follows a forward modeling procedure using time domain deconvolution techniques [e.g., *Ammon*, 1991]. Receiver functions are normalized to 1.0 and stacked to further amplify consistent P-to-S conversions. Evidence of azimuthal dependence suggested by the Cascadia earthquake receiver function was not resolvable using this dataset [*DeShon*, 2004], and we stacked only the four cleanest $M_w \geq 6.0$ South America earthquakes for comparison with synthetic receiver functions (Figure 4). The first mid-amplitude arrival following the direct P occurs
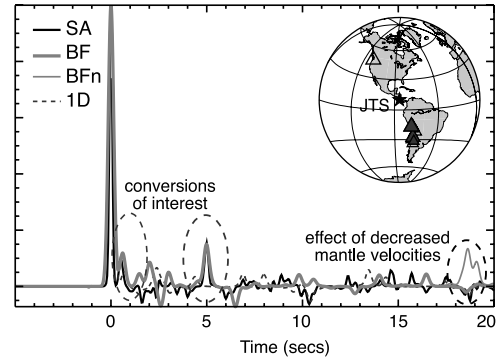

Figure 4. Receiver function modeling at JTS for teleseisms at $30-95°$ (triangles). The data stack (SA) uses only earthquakes from South America (filled triangles on inset). The Best Fit model (BF; model shown in Table 1) represents modifications to crustal velocity and density structure from *Sallarès et al.* [2001] that include reduced V_P between $32-40$ km depth. Model BFn represents the Best Fit model with normal mantle velocities (V_P: 8.1 km/sec; V_P/V_S: 1.78; density: 3.30 kg/m^3), and model 1D shows results computed through the Nicoya minimum 1D velocity model. The continental Moho can be modeled at $32-40$ km with little change in the resulting receiver function.

at ~ 5 secs (Figure 4), and a small Ps conversion at 1.0 sec is indicative of near-surface effects. The timing of major conversions does not vary if the Cascadia event is included.

[11] Synthetic vertical and radial waveforms are computed through horizontally layered 1D V_P, V_S, and density models and processed to create synthetic receiver functions. We test the Nicoya minimum 1D V_P and V_S models (Figure 2), the 1D approximation to 2D P-wave refraction data [*Sallarès et al.*, 2001], and a range of continental Moho depths, velocity contrasts, and density contrasts [see also *DeShon*, 2004]. The lack of multiple significant conversions out to 20.0 secs requires a fairly smoothly varying velocity structure reflecting velocity gradients rather than velocity contrasts (Figure 4). The 1D Nicoya velocity model predicts normal mantle velocities beneath 40 km depth but does not produce the conversion at ~ 5 secs (Figure 4). Slight modifications to the *Sallarès et al.* [2001] V_P and density model for northern Costa Rica, assuming V_P/V_S 1.78, accurately produce the 1.0 sec Ps conversion, the mid-amplitude 5.0 sec arrival, and low amplitude multiples (Figure 4). We test normal and serpentinized mantle wedge versions of the Best Fit model (BFn and BF in Figure 4; Table 1). Both synthetic 1D models based on P-wave refraction velocities match the 1 sec Ps conversion and

Table 1. Receiver Function Best Fit Model

Depth (km)	V_P (km/sec^2)	V_P/V_S	Density (kg/m^3)
0.0	5.30	1.78	2.75
4.0	5.90	1.78	2.75
6.5	6.10	1.78	2.95
11.0	6.40	1.78	2.95
16.0	6.70	1.78	2.95
21.0	6.80	1.78	3.00
25.0	6.95	1.78	3.00
29.0	7.20	1.78	3.00
32–40.0	7.40	1.85	3.10

the mid-amplitude conversion at 5 secs, which primarily results from the density contrast at 6.5 km depth. The normal mantle model predicts a large Moho multiple at ~18 secs that is not apparent on the stacked receiver function, and therefore the model with reduced P-wave velocities below $32-40$ km better fits the JTS receiver function. Best fit model modifications to *Sallarès et al.* [2001] include: 1) a 5% reduction in serpentinization leading to a slightly higher velocity contrast across the Moho; 2) a 0.5 km decrease in depth to the upper- and mid-crust density contrast; 3) a density reduction in the upper crust.

5. Conclusions

[12] Modeling of receiver functions, 1D, and 3D velocity in the Nicoya Peninsula region suggests a continental Moho depth of 36±4 km below sea level and forearc mantle wedge velocities of V_P $7.2-7.6$ km/sec and V_P/V_S ~1.85. These values are consistent with ~$15-25$% serpentinization of the mantle wedge [*Carlson and Miller*, 2003] and place Costa Rica in the middle range of serpentinization values currently cited [i.e., *Graeber and Asch*, 1999; *Kamiya and Kobayashi*, 2000; *Rondenay et al.*, 2001; *Seno et al.*, 2001]. All V_P models presented here are consistent with the compositional structure proposed by *Sallarès et al.* [2001] of a basaltic-gabbro mid-crust and mafic granulite lower crust, and the depth of the modeled Moho at JTS is consistent with the Moho depth reported using refraction data [*Sallarès et al.*, 2001]. The low velocity contrast from hydrated continental mantle to lower continental crust is not large, and when combined with effects of the subducting slab and station-data geometry, explains the range of continental Moho depths reported in Costa Rica and the associated error presented in this study.

[13] Station-data geometry does not allow us to determine the depth or landward extent of hydration within the continental mantle. Serpentinized mantle wedge near the subducting slab implies that rupture during large magnitude earthquakes will not initiate but may propagate along the oceanic slab/continental mantle interface making the downdip limit of the seismogenic zone beneath northern Costa Rica strain-rate dependent. Interplate seismicity ceases prior to the slab/continental mantle intersection (Figure 3) [*DeShon*, 2004], and interseismic seismicity does not illuminate the downdip limit of the seismogenic zone, similar to findings for the updip limit along this subduction segment [*Norabuena et al.*, 2004].

References

Ammon, C. J. (1991), The isolation of receiver effects from teleseismic P waveforms, *Bull. Seismol. Soc. Am.*, *81*, 2504–2510.

Carlson, R. L., and D. J. Miller (2003), Mantle wedge water contents estimated from seismic velocities in partially serpentinized peridotites, *Geophys. Res. Lett.*, *30*(5), 1250, doi:10.1029/2002GL016600.

DeShon, H. R. (2004), Seismogenic zone structure along the Middle America subduction zone, Costa Rica, Ph.D. thesis, 356 pp., Univ. of Calif., Santa Cruz.

Evans, J. R., D. Eberhart-Phillips, and C. H. Thurber (1994), User's manual for SIMULPS12 for imaging Vp and Vp/Vs: A derivative of the Thurber tomographic inversion SIMUL3 for local earthquakes and explosions, *U.S. Geol. Surv. Open File Rep., 94-431.*

Graeber, F. M., and G. Asch (1999), Three dimensional models of *P*-wave velocity and *P*-to-*S* velocity ratio in the southern central Andes from tomographic images of velocity and attenuation for *P* and *S* waves, *J. Geophys. Res.*, *104*, 20,237–20,256.

Husen, S., E. Kissling, E. Flüeh, and G. Asch (1999), Accurate hypocentre determination in the seismogenic zone of the subducting Nazca Plate in northern Chile using a combined on-/offshore network, *Geophys. J. Int.*, *138*, 687–701.

Husen, S., R. Quintero, E. Kissling, and B. Hacker (2003), Subduction-zone structure and magmatic processes beneath Costa Rica constrained by local earthquake tomography and petrological modeling, *Geophys. J. Int.*, *155*, 11–32.

Hyndman, R. D., and S. M. Peacock (2003), Serpentinization of the forearc mantle, *Earth Planet. Sci. Lett.*, *212*, 417–432.

Hyndman, R. D., M. Yamano, and D. A. Oleskevich (1997), The seismogenic zone of subduction thrust faults, *Island Arc*, *6*, 244–260.

Kamiya, S., and Y. Kobayashi (2000), Seismological evidence for the existence of serpentinized wedge mantle, *Geophys. Res. Lett.*, *27*, 819–822.

Kissling, E. (1988), Geotomography with local earthquakes, *Rev. Geophys.*, *26*, 659–698.

Kissling, E., and J. C. Lahr (1991), Tomographic image of the Pacific Slab under southern Alaska, *Eclogae Geol. Helv.*, *84*, 297–315.

Kissling, E., U. Kradolfer, and H. Maurer (1995), VELEST user's guide-short introduction, report, Inst. of Geophys. and Swiss Seismol. Serv., Zurich, Switzerland.

Matumoto, T., M. Othake, G. Latham, and J. Umaña (1977), Crustal structure of southern Central America, *Bull. Seismol. Soc. Am.*, *67*, 121–134.

Norabuena, E., et al. (2004), Geodetic and seismic constraints on some seismogenic zone processes in Costa Rica, *J. Geophys. Res.*, *109*, doi:10.1029/2003JB002931, in press.

Protti, M., et al. (1995), The March 25, 1990 (M_W = 7.0, M_L = 6.8), earthquake at the entrance of the Nicoya Gulf, Costa Rica: Its prior activity, foreshocks, aftershocks, and triggered seismicity, *J. Geophys. Res.*, *100*, 20,345–20,358.

Protti, M., S. Y. Schwartz, and G. Zandt (1996), Simultaneous inversion for earthquake location and velocity structure beneath central Costa Rica, *Bull. Seismol. Soc. Am.*, *86*, 19–31.

Quintero, R., and F. Güendel (2000), Stress field in Costa Rica, Central America, *J. Seismol.*, *4*, 297–319.

Quintero, R., and E. Kissling (2001), An improved P-wave velocity reference model for Costa Rica, *Geofís. Int.*, *40*, 3–19.

Quintero, R., and O. Kulhanek (1998), Pn-wave observations in Costa Rica, *Geofís. Int.*, *37*, 171–182.

Rondenay, S., M. G. Bostock, and J. Shragge (1993), Multiparameter two-dimensional inversion of scattered teleseismic body waves: 3. Application to the Cascadia 1993 data set, *J. Geophys. Res.*, *106*, 30,795–30,807.

Sallarès, V., J. J. Dañobeitia, and E. R. Flüeh (2000), Seismic tomography with local earthquakes in Costa Rica, *Tectonophysics*, *296*, 61–78.

Sallarès, V., J. J. Dañobeitia, and E. R. Flüeh (2001), Lithospheric structure of the Costa Rican Isthmus: Effects of subduction zone magmatism on an oceanic plateau, *J. Geophys. Res.*, *106*, 621–643.

Scholz, C. H. (1998), Earthquakes and friction laws, *Nature*, *391*, 37–42.

Seno, T., D. Zhao, Y. Kobayashi, and M. Nakamura (2001), Dehydration of serpentinized mantle: Seismic evidence from southwest Japan, *Earth Planets Space*, *53*, 861–871.

von Huene, R., C. R. Ranero, W. Weinrebe, and K. Hinz (2000), Quaternary convergent margin tectonics of Costa Rica: Segmentation of the Cocos Plate and Central American volcanism, *Tectonics*, *19*, 314–334.

Yao, Z. S., R. Quintero, and R. G. Roberts (1998), Tomographic imaging of P- and S-wave velocity structure beneath Costa Rica, *J. Geodyn.*, *3*, 177–190.

Zhao, D., A. Hasegawa, and S. Horiuchi (1992), Tomographic imaging of P and S wave velocity structure beneath northeastern Japan, *J. Geophys. Res.*, *97*, 19,909–19,928.

————————————

H. R. DeShon and S. Y. Schwartz, Earth Science Department, University of California, Santa Cruz, 1156 High Street, Santa Cruz, CA 95064, USA. (hdeshon@es.ucsc.edu)